An iceberg forecast approach based on a statistical ocean current model ☆

Leif Erik Andersson[a,*], Francesco Scibilia[a,b], Lars Imsland[a]

[a] *Department of Engineering Cybernetics, Norwegian University of Science and Technology, 7491 Trondheim, Norway*
[b] *Statoil ASA, Statoil Research Center, Arkitekt Ebbells veg 10, 7053 Ranheim, Norway*

Abstract

This article proposes a statistical model for short-term iceberg drift forecasts by transforming the problem of forecasting the iceberg velocity into a problem of forecasting the ocean current velocity. A Vector-autoregression model is identified using historical ocean current data as a training set. The proposed forecast scheme is tested and analysed on four real iceberg drift trajectories. Based on these results, recommendations about the forecast horizon, the filter horizon and model order are given. Moreover, it is shown that the statistical forecast approach presented in this article offers superior performance to a conventional dynamic iceberg forecast model for short-term drift forecasts.

Keywords: Iceberg drift forecasting, offshore operations, parameter estimation, multivariate empirical mode decomposition, moving horizon estimator, model identification

1. Introduction

Short-term iceberg drift forecast is challenging due to large uncertainties in the driving forces and model parameters.

A simple mechanistic dynamic iceberg drift model was developed in the 1980's (Sodhi and El-Tahan, 1980) and further improved and tested for short-term (< 24 h), intermediate-term (1 days to 3 days) and long-term (> 1 month) forecast by among others Mountain (1980); EI-Tahan et al. (1983); Smith (1993); Bigg et al. (1996); Kubat et al. (2007); Eik (2009); Turnbull et al. (2015); Kulakov and Demchev (2015). These models use the following set or subset of inputs: Environmental inputs (winds, waves and currents) and a detailed description of the iceberg keel geometry to simulate iceberg drift. However, predicting problematic iceberg trajectories that approach vulnerable offshore structures and development activities is still not solved to a completely satisfying extent.

Ocean current direction and speed are often identified as the most uncertain iceberg drift model forcings (Eik, 2009; Turnbull et al., 2015; Kubat et al., 2005; Broström et al., 2009). They introduce significant uncertainties into the iceberg drift forecast and make an accurate forecast very challenging (Allison et al., 2014). Even though the main drift direction of operational iceberg models are claimed to be satisfactory (Mountain, 1980; Kubat et al., 2005; Bigg et al., 1997), the modelled and observed iceberg trajectories may deviate from the beginning of the forecast and may even point in opposite directions (EI-Tahan et al., 1983). The process noise (the difference between the modelled and real driving forces) plays an important role during the forecast and gives the forecaster a feeling that the iceberg drift follows a "chaotic" behaviour.

In an operational setting a conventional dynamic iceberg drift forecast may provide an occupancy grid map with information on how many icebergs occupy each grid cell. Once an iceberg is discovered by satellite imagery or a direct sighting by aeroplane or ship, it is included in the occupancy grid map. Each iceberg trajectory is forecasted with the help of current, wind and wave models. The iceberg deterioration is usually also modelled. Icebergs are removed from the grid map if the deterioration model suggests with some conservatism that the iceberg is melted completely.

Available information about icebergs is often limited. The iceberg position is updated infrequently and limited to no initial information about the iceberg shape or initial velocity may be available. In such a situation, the only option to forecast the iceberg trajectory is to use the mechanistic dynamic iceberg model. In contrast, an iceberg approaching an offshore platform may be tracked continuously by e.g. marine radars.

In this situation, other approaches that include past information to forecast an iceberg trajectory are feasible (Andersson et al., 2018). In this article a simple transformation is introduces that allows to forecast the iceberg trajectory with a statistical ocean current model. On several iceberg trajectories the usefulness of the approach is analysed and tested.

The article proceeds as follows: Section 2 motivates the use of statistical ocean models in iceberg drift forecast. The methods and theory used in this article are

☆This work was supported by Statoil ASA, and in part by Centre for Autonomous Marine Operations and Systems (CoE AMOS, RCN project no. 223254). The study has been conducted using E.U. Copernicus Marine Service Information.

*Correspondence should be addressed to Leif Erik Andersson: e-mail: leif.e.andersson@ntnu.no; tel.: +47 735 94 365

introduced in Section 3. The performance indices used to evaluate the iceberg forecast are described in Section 4. The dataset used in this article is introduced in Section 5. A pre-analysis of the dataset is presented in Section 6, before the forecast scheme is tested on four iceberg drift trajectories in Section 7. The article ends with a conclusion in Section 8.

2. Motivation

It has been observed that for the short-term forecasts (1 h to 24 h) of iceberg trajectories that methods incorporating past observations exhibit superior performance relative to simulations of mechanistic dynamic models (Andersson et al., 2018; Marko et al., 1988). This is not surprising since they work with more information. Many mechanistic dynamic model approaches to iceberg forecasting use only some prior information and a process model to forecast the iceberg trajectory and they do not correct their model with measurements often due to a lack of this information.

A major issue for the iceberg drift forecast problem are the limited datasets. Only for a handful of icebergs are the keel shape, drift trajectory, and current close to the iceberg measured and analysed. Even in such idealistic conditions, it was not always possible to forecast or even hindcast the iceberg trajectory with the given dataset (Smith and Donaldson, 1987; Andersson et al., 2017).

The actual iceberg drift model and its noise distribution was never sufficiently analysed to conclude how well the model is able represent the iceberg drift. The most systematic approach towards this goal was performed by (Garrett, 1985; Moore, 1987) who analysed the correlation between iceberg, wind and current velocity. An attempt to capture the uncertainty in the dynamic model by describing the uncertainties of the parameters with several distributions was done by Allison et al. (2014). We believe that the performance and uncertainty of the iceberg model will depend on the iceberg location and how well the currents and winds are represented by the environmental models at a specific location. The iceberg trajectories, however, represent a Lagrangian particle flow where the observer moves with the particle. Consequently, a significant number of iceberg trajectories passing through the same area has to be available to find location-specific noise distributions. As of today, these data are not available and not feasible to receive. New satellite programs from the European, American or other space agencies may improve the situation in the future.

This article chooses another way to overcome the lack of iceberg drift data. The idea is to use the well-known kinematic relationship between iceberg, ocean current, and wind velocities

$$\mathbf{v}^i = \mathbf{v}^w + \alpha \mathbf{v}^a, \tag{1}$$

where $\mathbf{v}^i$, $\mathbf{v}^w$, and $\mathbf{v}^a$ are the iceberg, ocean current and wind velocity, respectively. The parameter α is about 0.017 to 0.02 (Smith, 1993; Bigg et al., 1997; Garrett et al., 1985). This empirical relationship was also recently derived analytically (Wagner et al., 2017). The central assumptions in the derivation by Wagner et al. (2017) are:

- Steady-state,
- Approximation of the pressure gradient force by the ocean velocity $\mathbf{v}^w$,
- Much smaller iceberg velocity $\mathbf{v}^i$ than wind velocity $\mathbf{v}^a$,
- Neglecting forcing due to sea ice and wave radiation,
- Neglecting vertical variations of the ocean current over the iceberg keel.

In addition, we assume that the uncertainty in the current dominates the uncertainty in the wind forecast. Consequently, with frequent iceberg position measurements (Eq. 1) can be used to estimate the ocean current velocity[1]. This transfers the problem of predicting the iceberg velocity to a problem of predicting the current velocity at a specific location. Moreover, in principle the uncertainties of the iceberg drift forecast can be approximated with the uncertainties of the current prediction model. The advantage of this transmission is that sufficient current velocity data are available to identify a statistical current model for short-term predictions. This model can then be used for further analysis.

3. Theory and Methods

3.1. The Vector-Autoregression model and Granger's causality

As motivated in the previous section the ocean current data are analysed. Eventually a model from the ocean current data is identified that helps to predict the iceberg movement. In this article we will identify a Vector-Autoregression model (VAR-model).

An important model identification step is to identify causality between input and output variables of the model. Granger's causality (G-causality) is used, since it is frequently used, simple to implement, and offers sufficient performance for the scope of this article.

A variable $\mathbf{u}_2$ is said to G-cause a variable $\mathbf{u}_1$ if the past of $\mathbf{u}_2$ contains information that helps to predict the future of $\mathbf{u}_1$ over and above information already in the past of $\mathbf{u}_1$ (Granger, 1969). In our case $\mathbf{u}_1$ may be, for example, the

[1] Also the dynamic iceberg model can be used to estimate the current velocity given iceberg position measurements. The advantage of using (Eq. 1) is that the model has only one parameter.

current velocity and $\mathbf{u}_2$ the wind velocity.

If we combine this with an estimated Vector-Autoregression model (VAR-model), then the simplest unconditional G-causality can be motivated as follows (Barnett and Seth, 2014):

Suppose $\mathbf{u}_k$ can be split into two jointly distributed multivariate processes

$$\mathbf{u}_k = \begin{pmatrix} \mathbf{u}_{1,k} \\ \mathbf{u}_{2,k} \end{pmatrix}. \tag{2}$$

As a VAR formulation, the model of this vector can be denoted as

$$\mathbf{u}_k = \sum_{i=1}^{p} \mathbf{A}_i \mathbf{u}_{k-i} + \boldsymbol{\varepsilon}_k \tag{3a}$$

$$\begin{pmatrix} \mathbf{u}_{1,k} \\ \mathbf{u}_{2,k} \end{pmatrix} = \sum_{i=1}^{p} \begin{pmatrix} \mathbf{A}_{11,i} & \mathbf{A}_{12,i} \\ \mathbf{A}_{21,i} & \mathbf{A}_{22,i} \end{pmatrix} \begin{pmatrix} \mathbf{u}_{1,k-i} \\ \mathbf{u}_{2,k-i} \end{pmatrix} + \begin{pmatrix} \boldsymbol{\varepsilon}_{1,k} \\ \boldsymbol{\varepsilon}_{2,k} \end{pmatrix}, \tag{3b}$$

where the matrices $\mathbf{A}_i$ are the regression coefficients, $\boldsymbol{\varepsilon}_k$ the residuals and p is in this article referred to be the model order. The residual covariance matrix is denoted as

$$\Sigma_{\mathbf{u}_1\mathbf{u}_1} = cov \begin{pmatrix} \boldsymbol{\varepsilon}_{1,k} \\ \boldsymbol{\varepsilon}_{2,k} \end{pmatrix} = \begin{pmatrix} \boldsymbol{\Sigma}_{11} & \boldsymbol{\Sigma}_{12} \\ \boldsymbol{\Sigma}_{21} & \boldsymbol{\Sigma}_{22} \end{pmatrix}. \tag{4}$$

The parameters of the VAR-model are fitted by solving an optimisation problem, e.g. ordinary least squares (Barnett and Seth, 2014).

The $\mathbf{u}_1$-component of the regression (3) is

$$\mathbf{u}_{1,k} = \sum_{i=1}^{p} (\mathbf{A}_{11,i}\mathbf{u}_{1,k-i} + \mathbf{A}_{12,i}\mathbf{u}_{2,k-i}) + \boldsymbol{\varepsilon}_{1,k} \tag{5}$$

from which we see that the dependency of $\mathbf{u}_1$ on the past of $\mathbf{u}_2$, given its past, is encapsulated in the coefficients $\mathbf{A}_{12,i}$. If these coefficients are zero, there is no conditional dependency on the past of $\mathbf{u}_2$. These lead to the reduced regression, which omits the past of $\mathbf{u}_2$

$$\mathbf{u}_{1,k} = \sum_{i=1}^{p} \mathbf{A}_{11,i}\mathbf{u}_{1,k-i} + \hat{\boldsymbol{\varepsilon}}_{1,k}, \tag{6}$$

so that $\mathbf{u}_{1,k}$ is predicted by its past only. The covariance matrix of the reduced regression is denoted as $\hat{\Sigma}_{11} \equiv cov(\hat{\boldsymbol{\varepsilon}}_{1,k})$.

The G-causality from $\mathbf{u}_2$ to $\mathbf{u}_1$ is defined to be the log-likelihood ratio

$$\mathcal{F}_{\mathbf{u}_2 \to \mathbf{u}_1} \equiv \ln \frac{|\hat{\Sigma}_{11}|}{|\Sigma_{11}|}, \tag{7}$$

comparing the information content of the full (Eq. 3) and the reduced regression (Eq. 6). Thus, G-causality quantifies the reduction in the prediction error when the past of the process $\mathbf{u}_2$ is included in the explanatory variables of the VAR model of $\mathbf{u}_1$.

3.1.1. Bayesian Information Criterion

The determination of the necessary model order for the VAR current model (Eq. 3) is done with the Bayesian Information Criterion (BIC). This is a model selection method that penalises the maximum likelihood criteria with the amount of parameters used in the fitted model. It has a single component that quantifies the goodness-of-fit, for example, through maximum likelihood, and one component that discounts the goodness-of-fit by the degree to which it was accomplished using a complex model:

$$BIC = -2 \ln f(\mathbf{U}|\hat{\theta}) + d \ln(n), \tag{8}$$

where d refers to the number of free parameters, n refers to sample size, and $\hat{\theta}$ refers to the maximum likelihood estimate. According to this criterion the model with the lowest BIC is the best.

3.2. Multivariate empirical mode decomposition

The multivariate empirical mode decomposition (MEMD) is a fully data-driven adaptive signal processing method. The MEMD is an extension to multivariate signals of the empirical mode decomposition (EMD). The EMD decomposes a signal $\mathbf{u}(t)$ into amplitude- and/or frequency modulated components called intrinsic mode functions (IMFs) $\mathbf{c}_l(t)$ and a bias term $\mathbf{r}(t)$, such that

$$\mathbf{u}(t) = \sum_{l=1}^{N} \mathbf{c}_l(t) + \mathbf{r}(t). \tag{9}$$

More details about the MEMD can be found in Ur Rehman and Mandic (2010).

In this article the MEMD will be used in the analysis to remove high frequency components (lower IMFs) from the ocean current data. This guarantees that the analysis is not corrupted by high frequency components. Moreover this filtering method prevents a phase shift as, for instance, exhibited by a moving average filter. In addition, high frequency components of the iceberg dynamics can be added after a forecast step, if only slow frequency components are forecasted.

4. Performance indices

The performance of the iceberg forecast is measured directly with the mean $\hat{\zeta}$ of the end position error $\zeta = |\hat{\boldsymbol{\chi}}_{end} - \boldsymbol{\chi}_{end}|$ of all forecasts performed where $\hat{\boldsymbol{\chi}}_{end}$ and $\boldsymbol{\chi}_{end}$ are the end positions of the forecasted and measured iceberg drift trajectories.

Moreover, a relative performance index is introduced to compare the different forecast models on different icebergs (Andersson et al., 2018). It may be that the icebergs drift considerably differently (for instance, with different drift velocities). These may result in a larger mean and median error compared to slow icebergs. The relative forecast error is defined as

$$|\boldsymbol{\chi}_{end} - \hat{\boldsymbol{\chi}}_{end}| < \kappa |\boldsymbol{\chi}_{end} - \boldsymbol{\chi}_{init}|, \tag{10}$$

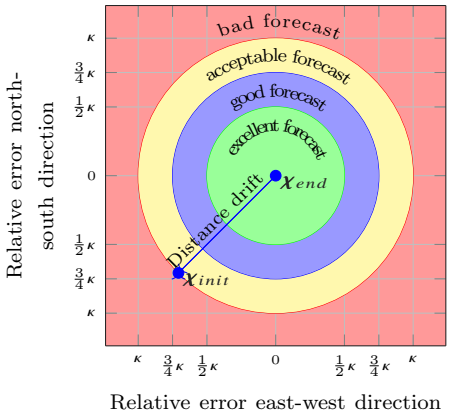

Figure 1: Visualisation of the relative performance index (Andersson et al., 2018). If the end position of the iceberg forecast is encapsulated in the inner circle is defined as excellent, followed by two rings where the forecast is defined good and acceptable. If the forecast is not encapsulated by the outer circle is defined as bad.

where $\boldsymbol{x}_{init}$ is the initial position of the measured iceberg trajectory. The value κ is a performance index. For this article, the following forecast categories are chosen (Fig. 1):

- Bad forecast: $\kappa > 1$,
- Acceptable forecast: $1 \geq \kappa > 0.75$,
- Good forecast: $0.75 \geq \kappa > 0.5$,
- Excellent forecast: $\kappa < 0.5$.

The relative performance index has a singularity if the actual iceberg trajectory describes a closed loop. In this case, every forecast will be classified as bad.

5. Dataset

5.1. Iceberg Data

The icebergs were discovered during the Offshore Newfoundland Research Expedition conducted by Statoil and ArticNet (ArcticNet, 2004-2018) on April 22th and 24th 2015 (Fig. 2). The International Ice Patrol classification C-CORE (2007) is used to categorize the iceberg shapes. One GPS beacon was deployed on Iceberg 1 and Iceberg 2, four GPS beacons were deployed on Iceberg 3. The beacons provided (at least) hourly position updates. From Iceberg 1 about eight days, from Iceberg 2 about four days, and from Iceberg 3 about 37 days of iceberg drift data are available (Tab. 1). A special situation occurred for Iceberg 3. It broke into two pieces after about 5.5 days. The difference in drift direction between both iceberg pieces after the separation is about 60°. For the (most likely) smaller piece (Iceberg 3-2) about 52 days of drift data are available. The drift trajectories of all icebergs are shown in Fig. 3.

The datasets of Iceberg 1 and Iceberg 2 are relatively small. The icebergs were only observed for a short period before the GPS signal was lost. The dataset of Iceberg 3 and Iceberg 3-2 are sufficiently long. However, the size of Iceberg 3-2 is probably small, which may be the reason for the strong and quick drift direction changes.

Iceberg 1 and Iceberg 2 drifted in close proximity to each other. However, the drift behaviour is quite different. Iceberg 1 drifted southwards, made several loops before it drifted towards the west. Iceberg 2 drifted mainly towards the west. After Iceberg 3 and Iceberg 3-2 separated, Iceberg 3-2 drifted into south-west directions, entered several loops and directions changes before it drifted into east and north direction. Iceberg 3, on the other hand, drifted first into west direction, made a large curve and drifted afterward into south direction (Fig. 3).

5.2. Current Data

The current dataset was received from the E.U. Copernicus Marine Service, and the Global Ocean 1/12° Physics Analysis and Forecast model was used. The Operational Mercator global ocean analysis and forecast system at 1/12° provides ten days of 3D global ocean forecasts that are updated daily. More specifically, in this article the one-hour surface current and daily mean depth average current information are used. For two different areas, the current was extracted from the global model. One area is constrained within 49.5° to 53° latitude and −54.5° to −47.5° longitude, and the other is within 48.0° to 49° latitude and −54° to −52° longitude. The first results are within an approximate 400×500 km large grid with 85×43 (Lon×Lat) grid cells and the second within an approximate 110×150 km large grid with 25×13 grid cells. These are the two areas of interest where the icebergs discussed in this research were tracked. In both cases, the one year of current data are used to identify the ocean current model equivalent to 8760 time points.

Figure 4, the iceberg drift directions can be compared with the yearly mean surface current directions. It is not expected that the iceberg drifts with the mean current direction, but the mean current can give valuable insights about the local current regime.

Both the drift direction of Iceberg 1 and Iceberg 2 do not correlate well with the mean current direction. The drift direction of Iceberg 3, on the other hand, correlates relatively well with the mean current direction. Again, the drift direction of Iceberg 3-2 does not correlate well with the mean current. It can, however, be observed that the iceberg drift directions change more often in areas with diverse current regimes (i.e., it seems more "variable" in these regions) (Fig. 4).

5.3. Wind Data

The wind data were also received from the E.U. Copernicus Marine Service. The blended global ocean mean wind fields are used and are estimated from scatterometer retrievals. They have a horizontal resolution of 0.25°×0.25° and are updated every 6 h. Since the grid cells are larger,

(a) Iceberg 1 on April 22, 2015 - Shape: Dry dock.

(b) Iceberg 2 on April 22, 2015 - Shape: Rounded.

(c) Iceberg 3 on April 24, 2015 - Shape: Wedged.

Figure 2: Iceberg from several sides

Table 1: Iceberg data set. The iceberg geometries are from the day of the GPS beacon deployment.

	Iceberg shape	**horizontal dimensions** [m]	**freeboard** [m]	**keel depth** [m]	**measurement frequency** [h]	**drift data** [days]	**GPS tracker**
Iceberg 1	dry-dock	210 × 150	30	45 – 60	1	8	Canatec
Iceberg 2	rounded	100 × 100	16	75	1	4	Canatec
Iceberg 3	wedged	290 × 100	30	90 – 100	1	37	2 Canatec & 2 (1) Solara
Iceberg 3-2	–	–	–	–	1	52	Solara

fewer cells are necessary to cover the region, which results in a 29×15×1460 and 9×5×1460 (Lon×Lat×time) large grid. The wind data is linearly interpolated onto the current data in time and location. Possible empty data points were removed from the dataset.

6. Pre-Analysis

6.1. Time horizon of kinematic models

6.1.1. Current data

An important parameter for the operational iceberg forecast is the time horizon for which kinematic models are reliable. For this, the auto-correlation of the current-velocity, current-acceleration, and higher derivatives (also called moments) are compared to their future values. As the current-data come from a model, which contains smoothed data, it can only give an upper bound on how long the derivative of the position may be correlated.

The joint probability density functions $p(\mathbf{x}_i|\mathbf{x}_{i-t})$ are plotted. As long as these probability density functions contain some structure, a model could exploit the structure and improve the forecast. In contrast, when no structure can be detected, the initial information about the moment is completely degraded to Gaussian noise. If this state is reached, then a kinematic model assuming, for example, constant velocity or constant acceleration is no longer beneficial. In fact, the most likely value for the considered moment would be zero.

To analyse the correct frequency range, high frequencies within the targeted forecast horizon t_h must be removed from the dataset. These frequencies can corrupt the analysis performed here considerably by adding additional change to the current velocity and its derivatives. Therefore, these frequencies (tidal and inertial frequencies) are removed with the help of the MEMD. The IMFs containing oscillations with a period of less than 30 h were removed (the intention was to eliminate oscillations with a period smaller than 24 h, and we added a 6 h-buffer). The remaining IMFs and the bias were added up to represent the smoothed dataset (Fig. 5).

The example shown here represents one grid cell, but similar observations were also obtained for the other grid cells. It can be seen that over time the correlation between initial and actual velocity decreases (Fig. 6). On the other hand, it can also be observed that a model assuming constant velocity will be approximately correct in the first hours. Even though a correlation after 24 h can still be detected, the variance is significant, introducing a considerable uncertainty into the model that only assumes constant velocity.

The auto-correlation of the acceleration is shown in Figure 7, which shows the variance of the joint probability

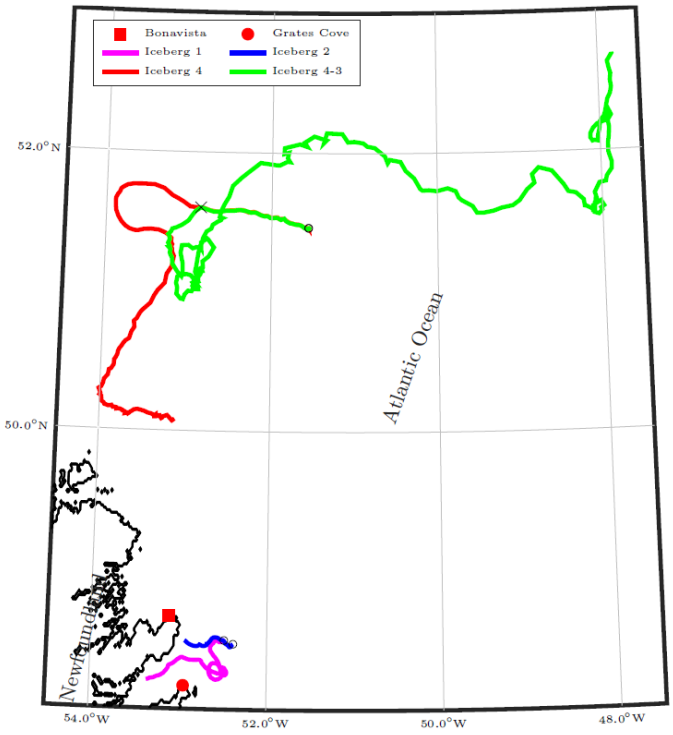

Figure 3: Map of iceberg drift trajectories. Iceberg 1 and Iceberg 2 are close to the shoreline of Newfoundland while Iceberg 3 and Iceberg 3-2 drift on the open ocean. The initial positions of the icebergs are marked with a circle and the location where the Iceberg 3 broke with a cross. For better recognition the weather station in Bonavista is marked on the map.

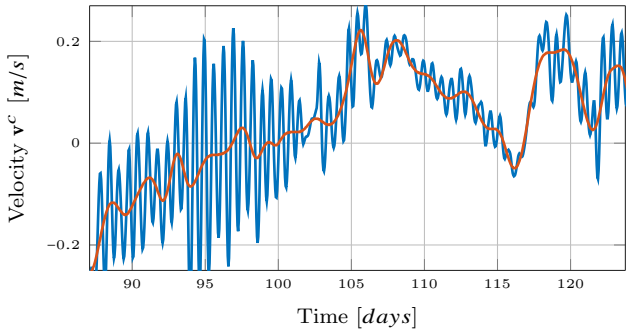

Figure 5: Example for current velocity and smoothed current velocity profile.

distribution of a 1 h interval is relatively small. Thus, the uncertainty of a model assuming constant acceleration is also small. On the other hand, after 6 h the joint probability distribution approaches a Gaussian distribution, and after 12 h the joint probability distribution is Gaussian. The structure which we would like to exploit during the forecast is vanished. Moreover, after 24 h we can even detect a linear structure opposite to the one observed for the smaller intervals. Hence, for extreme acceleration values, it is more likely to change sign than stay constant.

To conclude, it can be seen that the diffusion due to process noise of the acceleration is nearly complete after 12 h, and only minimal information remains from the initial acceleration.

For the higher derivatives, the correlation between initial and future values decreases further. It is, therefore, unlikely that kinematic models based on higher-order derivatives are beneficial, especially considering that filtered and unsmoothed data are used in a real forecast scenario, which will further decrease the correlation. If a filter horizon t_f of 12 h is used, then the acceleration is Gaussian after about 7 h and the jerk[2] after 5 h.

6.1.2. Iceberg data

We analysed in the previous subsection the ocean current velocity and its derivatives, and we saw how the process noise quickly degrades the auto-correlation to Gaussian noise, especially for higher derivatives. To verify our assumption that a statistical ocean current model can be used to help with the iceberg forecast, we compare the forecast results of kinematic iceberg models assuming constant velocity or higher derivatives and integrating them to the iceberg position

$$\begin{pmatrix} \dot{\mathbf{x}}_1 \\ \vdots \\ \dot{\mathbf{x}}_{q+1} \end{pmatrix} = \begin{pmatrix} \mathbf{x}_2 \\ \vdots \\ 0 \end{pmatrix} \tag{11}$$

where $\mathbf{x}_1$ represents the velocity and $\mathbf{x}_2$ the acceleration. The kinematic model is assumed to be noise free. Considering the observation made in the previous section, the

[2] jerk $\hat{=}$ rate of change of acceleration

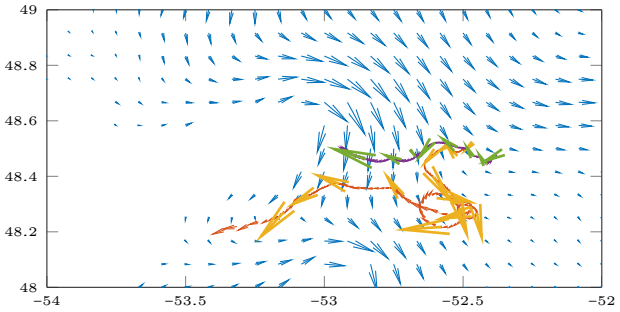

(a) Iceberg 1 and Iceberg 2.

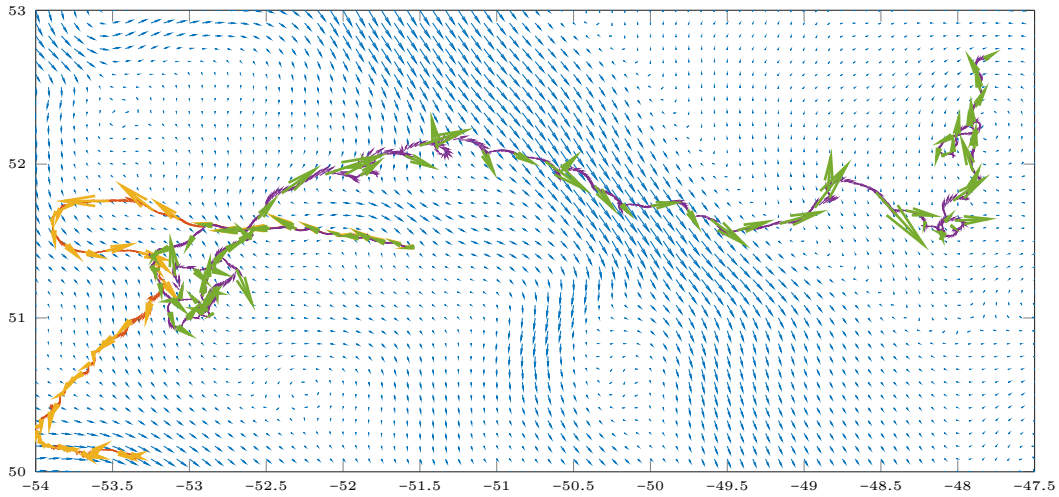

(b) Iceberg 3 and Iceberg 3-2.

Figure 4: Maps showing the yearly mean surface current. The arrows indicate the direction of the surface current in each grid cell. In addition, the iceberg drift trajectories and iceberg drift directions are plotted.

model should be limited to $q = 3$ (constant jerk), if not even $q = 2$ (constant acceleration)[3].

The forecast for different horizons using the simple kinematic model assuming either constant velocity, acceleration or jerk is shown in Figure 8. For every iceberg, the same pattern can be detected. In the first hours, higher-order models are beneficial. However, the simple constant velocity model has a similar performance. After about 9 h, the model assuming constant jerk performs worse than the lower-order models. The model assuming constant acceleration performs worse for Iceberg 1 and Iceberg 3-2 after about 10 h and for Iceberg 2 and Iceberg 3 after about 16 h. The reason for this behaviour was discussed in the previous subsection.

6.2. Cross-correlation of variables

In the previous subsection, it was shown that up to a certain order the current velocity derivatives are strongly auto-correlated. A simple auto-correlation model was proposed and tested on the iceberg dataset. Nevertheless, a statistical current model may be improved by also considering cross-correlations of the ocean current to other variables, such as wind velocities and the orthogonal current-velocity.

A Vector-Autoregression (VAR) model is identified using the MVGC Multivariate Granger Causality Toolbox

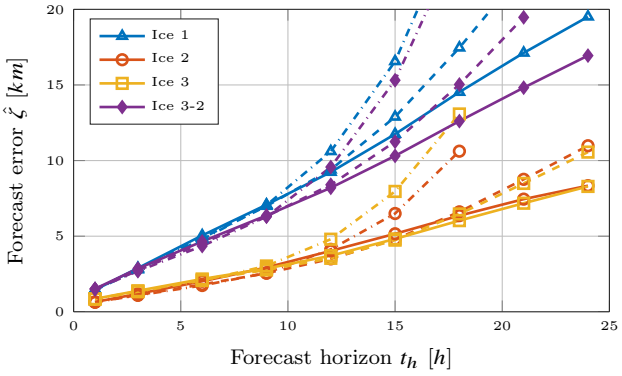

Figure 8: Mean forecast error $\hat{\zeta}$ of the iceberg drift forecast for different horizons t_h using different kinematic models. The solid lines assume constant velocity, dashed lines constant acceleration and dash-dotted lines constant acceleration change.

[3]There is a strong connection between the model order p of the VAR model and the order of derivatives q, e.g., the acceleration (q=2) can be calculated with two velocity points (p=2).

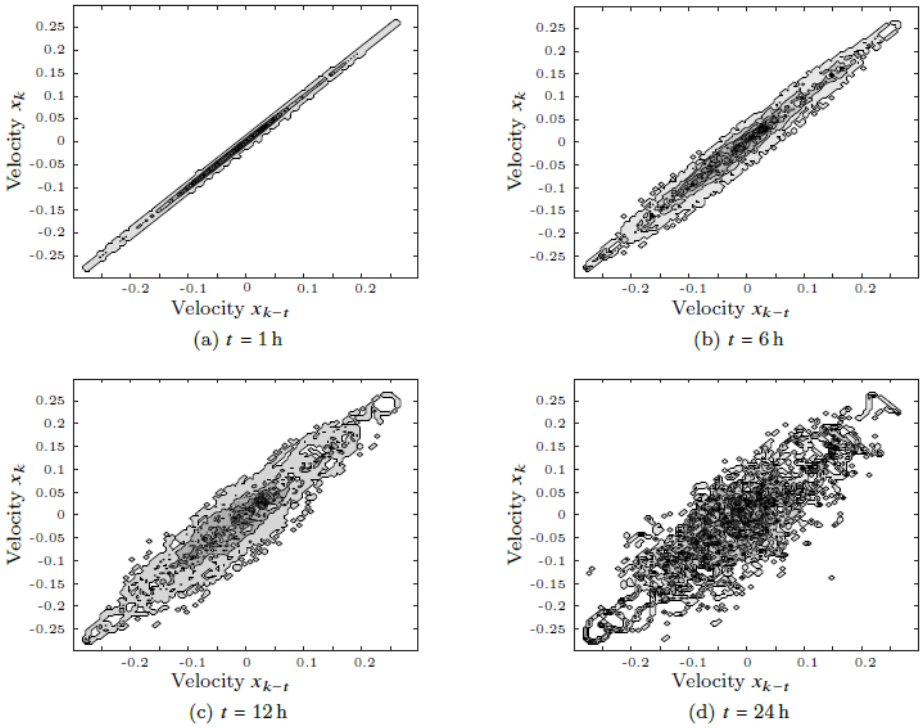

Figure 6: Joint probability mass functions of one current velocity profile for different intervals. The grey shading shows the likelihood.

(Barnett and Seth, 2014). An important prerequisite for model identification is the analysis of input and output correlations of the system. For this, Granger's causality is used. The analysis is performed on the original data, since pre-filtering may severely degrade Granger-causal inference and also increase the VAR model order (Barnett and Seth, 2014). Causality can be detected between orthogonal current velocities and same directed ocean current and wind velocities.

6.3. Optimal model order given by the BIC

As part of the G-causality analysis, a VAR model was fitted in the current data. Before this, the optimal model order was estimated by the BIC with a maximum model order restricted to $p = 20$ (see Eq. 3). In theory, we can identify a VAR model for each grid cell of the current grid, which improves the local characteristic of the iceberg drift. However, in this presentation, it was chosen to only identify two VAR models at the initial position of Iceberg 1 and Iceberg 3. The result of BIC for the two models is seen in Figure 9. The minimum for the BIC for Iceberg 3 is at a model order of $p = 17$, and $p = 15$ for Icebergs 1 and 2. However, the largest relative improvements are achieved within the first few model orders. In fact, the improvement from a first to a second order model is about 80 % of the total improvement. An additional increase to a third-order model gives 90 % of the overall improvement. Even though, the BIC suggests a higher-order model it is likely that already a low-order model can achieve adequate prediction results.

Algorithm 1 Iceberg drift forecast

Set $\hat{\boldsymbol{\chi}}_0 = \boldsymbol{\chi}$ and $k = 0$;
while Simulation horizon (t_s) ≤ Forecast horizon (t_h) **do**
  Get iceberg position $\hat{\boldsymbol{\chi}}_k$;
  Estimate iceberg velocity $\mathbf{v}_k^i$, e.g., with $\mathbf{v}_k^i = \frac{\hat{\boldsymbol{\chi}}_k - \hat{\boldsymbol{\chi}}_{k-1}}{t_k - t_{k-1}}$ (a filter to reduce measurement noise may be necessary);
  Estimate current velocity with $\mathbf{v}_k^c$ (Eq. 1);
  Take VAR model identified for grid cell closest to iceberg position;
  Calculate new current velocity $\hat{\mathbf{v}}_{k+1}^c$ with VAR model;
  Calculate new iceberg velocity $\hat{\mathbf{v}}_{k+1}^i$ with (Eq. 1);
  if High frequency components considered important **then** Add high frequency components that were removed using f.e. MEMD;
  end if
  Integrate to iceberg position $\hat{\boldsymbol{\chi}}_{k+1}$;
  Set k = k+1;
end while

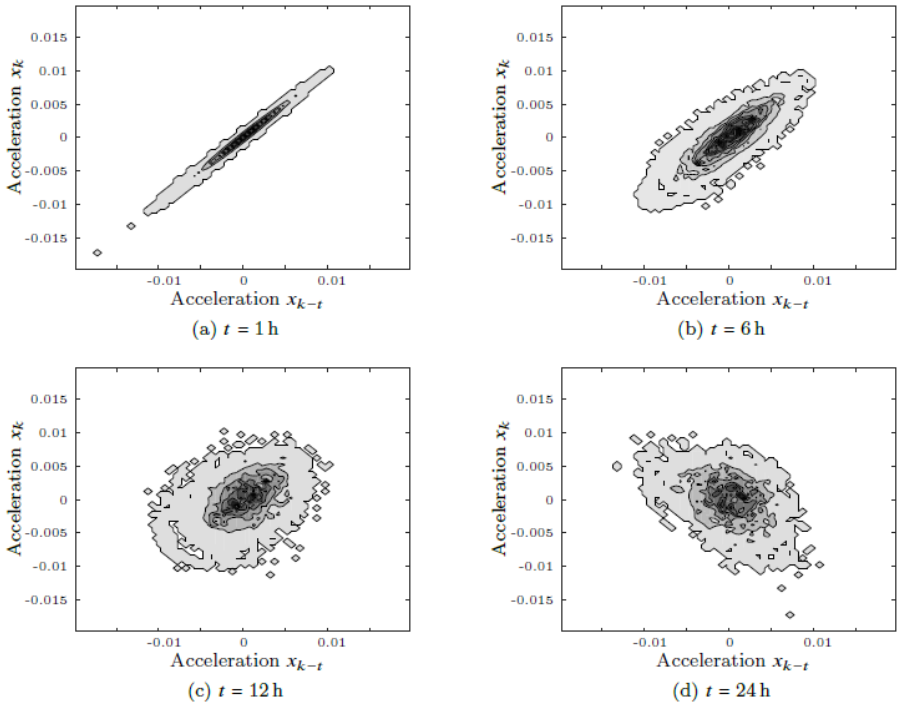

Figure 7: Joint probability mass functions of one current acceleration for different intervals. The grey shading shows the likelihood.

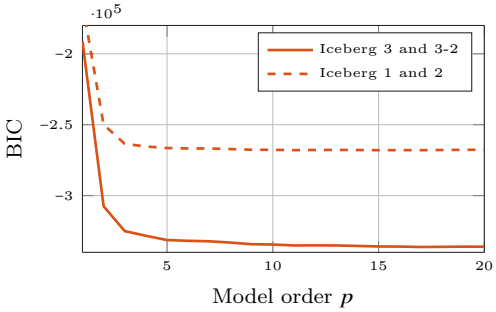

Figure 9: Value of Bayesian Information Criteria for model order up to $p = 20$. Solid line VAR model for Iceberg 3 and Iceberg 3-2 and dashed for Iceberg 1 and Iceberg 2.

7. Iceberg Forecast

In this section, the forecast of the iceberg trajectories using the identified VAR ocean current model are discussed. The forecast procedure, assuming that a VAR model was already identified, is given in Algorithm 1.

The forecast performance of different order VAR models, the influence of the filter, and the forecast horizon will be closely examined. Moreover, it is tested if the cross-correlations between north and east current velocity directions and same directed current and wind velocities are beneficial in the VAR model forecast of the ocean current[4].

[4]Wind information is used twice in Algorithm 1: Once to estimate the current velocity and the new iceberg velocity with eq. 1 and once in the VAR model forecast of the current velocity due to the cross-correlation between current and wind.

Both causalities were detected in the analysis and included into the model.

In the iceberg forecast case the iceberg velocity, which is used to estimate the current velocity, is influenced by measurement noise. In addition, the modelled current, which is used to identify the VAR model, is smoothed, so high-frequency changes are excluded from the modelled data. This is not the case for the iceberg velocity data. Therefore, the iceberg velocity data are filtered before every forecast step. A moving average filter is used, which presents a relatively small phase lag in comparison to other filters tested. Nevertheless, a time lag is present, which degrades the performance of the forecast. The robustness of the forecast to window sizes of the moving average filter is tested.

7.1. Model order for the iceberg forecast

The four icebergs were tested on VAR models of different orders. The BIC suggests an optimal model order of $p = 15$ to $p = 17$. The iceberg velocity is filtered with a 13 h moving average filter. A minimum position error for the different icebergs was detected at a model order $p = 3$. Larger model orders do not or only slightly improve the forecast (Iceberg 2). Overall, the VAR model order is not as sensitive to higher model orders as the simple kinematic model. The wind influence in the VAR model to forecast the ocean current velocity is small. The most considerable improvement for the iceberg forecast, if the ocean model includes a wind input, is observed for Iceberg 3-2. On the other hand, the forecast of Iceberg 3

improves if the wind input is neglected in the VAR ocean model.

7.2. Influence of moving horizon window length of the moving average filter

The moving average filter (or any other filter chosen) plays an important role in the forecast scheme. How robust the VAR model is against different filter lengths t_f is important. It indicates how robust the VAR model is to measurement noise and fast dynamics not represented in the training set used to identify the model. The third-order VAR model is used since it performed well when the different model orders were compared.

Figure 10 shows the mean errors $\hat{\zeta}$ of 12 h forecasts for the different icebergs including or excluding cross-correlation between orthogonal velocities.

The forecast performance of the VAR model differs between icebergs. While for Iceberg 2 and Iceberg 3, a minimum mean forecast error of about 3.2 km to 3.5 km can be reached, Iceberg 1 and Iceberg 3-2 have a minimum mean error at about 6 km to 7 km. If the cross-correlation between orthogonal current velocities is included in the model, then the optimal filter horizon t_f^{opt} is about 7 h to 10 h. If the cross-correlation is excluded then longer filter horizons are necessary. The optimum t_f^{opt} is about 13 h to 15 h. Moreover, if cross-correlation is excluded from the forecast, then it is more sensitive to small filter horizons, which is not observed if cross-correlation is included.

The drift trajectory of Iceberg 1 and Iceberg 3-2 have several loops. For these icebergs, it is beneficial to include cross-correlation between the orthogonal ocean current velocities. While the loops may not be forecasted precisely, every trajectory using this cross-correlation has a clockwise bend, which reduces the forecast error ζ if the iceberg trajectory loops clock-wise (which it usually does).

Overall, the mean end position errors changes only slightly around the optimal filter horizon t_f^{opt} indicating the models are robust. A conservative approach would be to use a longer filter horizon t_f.

7.3. Forecast horizon

The forecast horizon t_h in which recently measured information can be exploited to improve the forecast is limited. Figure 11 shows the mean end position error $\hat{\zeta}$ of the iceberg drift forecast using different forecast horizons t_h. Iceberg 2 was excluded from the figure because of the short dataset.

The error change with respect to the forecast horizon is defined as

$$\hat{\Gamma}(T_2) = \frac{\hat{\zeta}^{T_2} - \hat{\zeta}^{T_1}}{T_2 - T_1}, \tag{12}$$

where T_1 and T_2 describe the different length of the forecast horizons with $T_2 > T_1$.

The error change Γ has a minimum at $T = 12$ h. The iceberg drift is influenced by tidal currents, which have an oscillation period T of about 12 h and 24 h. Consequently,

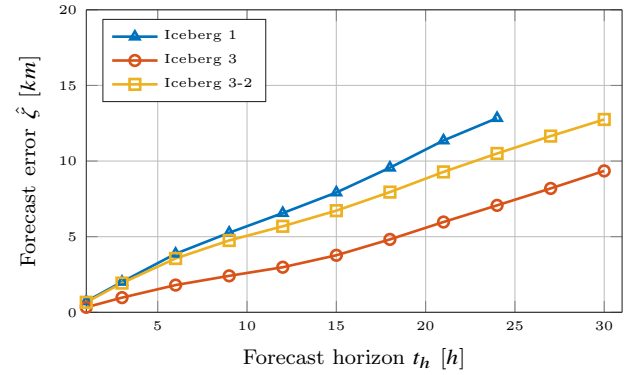

(a) Forecast error.

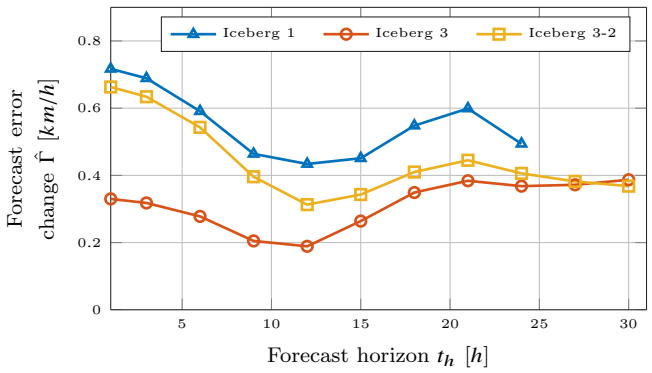

(b) Change of forecast error.

Figure 11: Mean $\hat{\zeta}$ forecast error for different forecast horizons t_h and change of the forecast error Γ for the third order VAR model.

these oscillations introduce the smallest error at multiples of $1/2T$. Therefore, the change of the forecast error is oscillating with the same frequency (Fig. 11). However, it can be detected that the error change Γ increases slightly over time.

It can be concluded that including measured information is beneficial for forecasts up to at least 12 h. Longer forecast may be possible, but will exhibit larger error growths Γ.

In the case of short forecast horizons t_h of about 1 h to 6 h, the filter horizon t_f should be in the range of about 1 h to 3 h. Afterward, the filter horizon t_f should be increased to the ranges discussed in the previous section.

7.4. First-order Model

The simplest VAR model to forecast the ocean current is the first order model

$$\mathbf{u}_k = \mathbf{A}\mathbf{u}_{k-1}. \tag{13}$$

In this case the wind influence in the VAR model to forecast the ocean current velocity is negligible, indicating that the wind mainly contributed to the ocean current acceleration in the higher order VAR models[5].

[5]The wind is still considered in the iceberg forecast through Eq. 1, but the cross-correlation between wind and current in the VAR model is negligible.

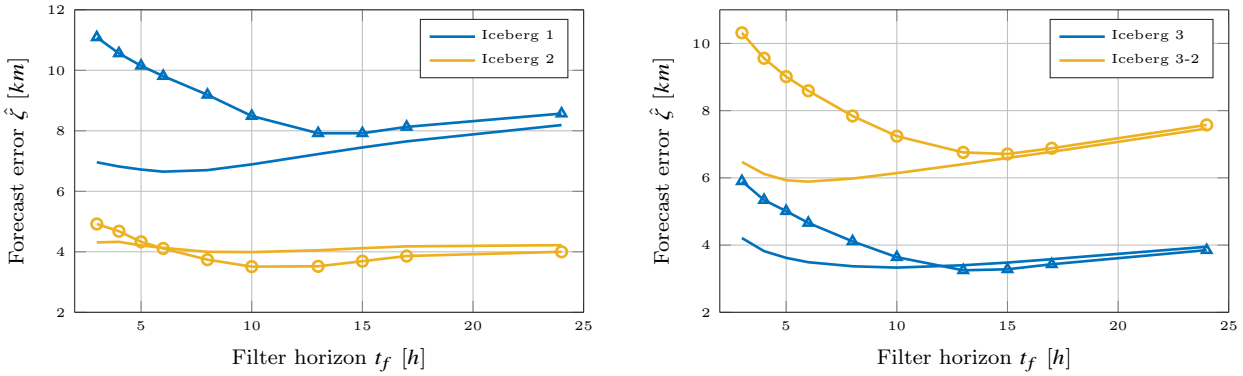

Figure 10: Mean forecast error $\hat{\zeta}$ for different filter horizons t_f with and without cross-correction between orthogonal velocities. Marked lines: without cross-correlation between orthogonal velocities.

The higher-order VAR models produce a slightly better 12 h forecast than the first-order VAR model (varying from 2 % reduction of the forecast error for Iceberg 3 to a 25 % reduction for Iceberg 1).

In comparison to the simple kinematic model assuming constant velocity (which is to some degree a first order model), the first-order VAR model provides a 3 % to 13 % better 12 h forecast. The improvement of the forecast with the first-order VAR model is due to the explicit consideration of the influence of the wind on the iceberg drift trajectory with Eq. 1 in the forecast algorithm (Alg. 1).

7.5. Dynamic Iceberg model

For comparison and to indicate the performance of the VAR ocean model, the icebergs are modelled with the dynamic iceberg drift model (Andersson et al., 2016). It is based on a momentum equation

$$m\mathbf{a} = \mathbf{f}_a + \mathbf{f}_c + \mathbf{f}_p + \mathbf{f}_{cor}, \tag{14}$$

where $\mathbf{a}$ is the iceberg acceleration and $\mathbf{f}_a$, $\mathbf{f}_c$, $\mathbf{f}_p$ and $\mathbf{f}_{cor}$ are the air drag, the water drag, the pressure gradient and Coriolis force, respectively. The total mass m of the iceberg consists of physical iceberg mass m_0 and added mass m_{add} ($m = m_0 + m_{add}$) due to the iceberg surrounding water field (Sodhi and El-Tahan, 1980).

The iceberg length, width, sail height, and keel depth were measured onsite and used in the model. Since a longer period is examined, a simple deterioration model is implemented assuming a daily 2 % deterioration of the iceberg length, width, draft, and sail height. This seemed reasonable as it allowed that Iceberg 3 and Iceberg 3-2 to be observed for such an extended period.

The iceberg mass is approximated using the shape coefficients for spherical, wedged, and dry-dock icebergs according to the International Ice Patrol (C-CORE, 2007). Iceberg 3 breaks apart after about 5.5 days. After evaluating the pictures of the iceberg, it is assumed that breakage happens at about 2/3 of the waterline length. Mass, width, draft, and sail are adjusted accordingly in the simulations. The two remaining icebergs are likely more dome-shaped than wedged. The shape factor is, therefore, adjusted after the breakage.

The iceberg is simulated using either the hourly surface current or the layered daily mean current provided by Copernicus Marine. Tidal current from the *Tidal Model Driver* (Egbert and Erofeeva, 2002) is added to the daily mean current to approximate the higher frequency components.

Two, one, and four surface drifters were deployed close to Iceberg 1, 2, and 3, respectively. The measured surface current velocity is compared to the modelled surface current received from the Copernicus Marine webpage. The model captures the overall current velocity (Fig. 12). The measured and modelled ocean currents are well correlated in some periods (0 h to 300 h and 600 h to 800 h), but in other they show obvious deviation (300 h to 400 h). The mean error in the north and east directions is about $5\,\mathrm{cm\,s^{-1}}$ and $1\,\mathrm{cm\,s^{-1}}$, respectively. The standard deviation in both directions is about $14\,\mathrm{cm\,s^{-1}}$. The absolute velocity is under-predicted by about $6\,\mathrm{cm\,s^{-1}}$. In addition, the measured current direction is more directionally distributed than the modelled one (Fig 13). The Copernicus Marine dataset considers grid cells of about 10×10 km, which smooths the current signal and reduces the amplitudes of the high frequency components.

Using a scatter diagram to investigate the modelled and measured current velocities, we find that a possible correction is

$$\begin{aligned} \tilde{v}^{c,n} &= 1.5 v^{c,n}, \\ \tilde{v}^{c,e} &= v^{c,e} - 0.05, \end{aligned} \tag{15}$$

where the superscripts stand for the north and east directions. This reduces the mean errors in both directions to zero and improves the directional distribution (Fig 13). However, the error in absolute velocity remains similar. We will continue using the original Copernicus ocean current data.

The iceberg keel shape is approximated using either a triangular, semi-elliptic or rectangular iceberg shape (Andersson et al., 2017). The triangular iceberg shape produces the smallest mean error $\hat{\zeta}$ for Iceberg 2, 3, and 3-2.

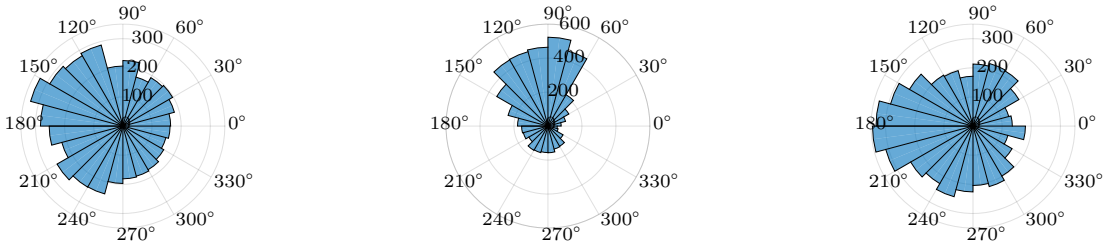

(a) Measured current. (b) Modelled current. (c) Corrected modelled current.

Figure 13: Directional distribution from measurements (a) versus directional distributions from the Copernicus Marine model (b) and corrected modelled current (c).

Table 2: Forecast error change $\hat{\Gamma}$ [km/h] of the dynamical, VAR and stationary model on the entire iceberg trajectories. Boldface is used to indicate the model with the smallest error growth.

		Change of mean error [km/h]								
		1 h	3 h	6 h	9 h	12 h	15 h	18 h	21 h	24 h
Ice 1	Dym. Mod.	**0.70**	0.87	0.86	0.77	0.72	0.71	0.71	0.67	0.63
	VAR Mod.	0.72	**0.69**	**0.59**	**0.46**	**0.43**	**0.45**	0.55	0.60	0.49
	Stat. Mod.	0.87	0.85	0.77	0.65	0.54	0.50	**0.51**	**0.49**	**0.47**
Ice 2	Dym. Mod	0.52	0.76	0.79	0.77	0.75	0.64	0.66	0.62	0.58
	VAR Mod.	**0.29**	**0.29**	**0.29**	**0.31**	**0.36**	**0.31**	**0.35**	**0.37**	**0.40**
	Stat. Mod.	0.46	0.45	0.45	0.47	0.50	0.29	0.44	0.46	0.49
Ice 3	Dym. Mod	0.38	0.57	0.63	0.63	0.63	0.65	0.63	0.62	0.61
	VAR Mod.	**0.33**	**0.32**	**0.28**	**0.20**	**0.19**	**0.26**	**0.35**	**0.38**	**0.37**
	Stat. Mod.	0.69	0.67	0.65	0.62	0.61	0.66	0.63	0.62	0.61
Ice 3-2	Dym. Mod	**0.65**	0.65	0.59	0.50	0.46	0.49	0.50	0.49	0.47
	VAR Mod.	0.66	**0.63**	**0.54**	**0.40**	**0.31**	**0.34**	**0.41**	**0.45**	**0.41**
	Stat. Mod	0.99	0.96	0.89	0.80	0.75	0.74	0.74	0.72	0.68

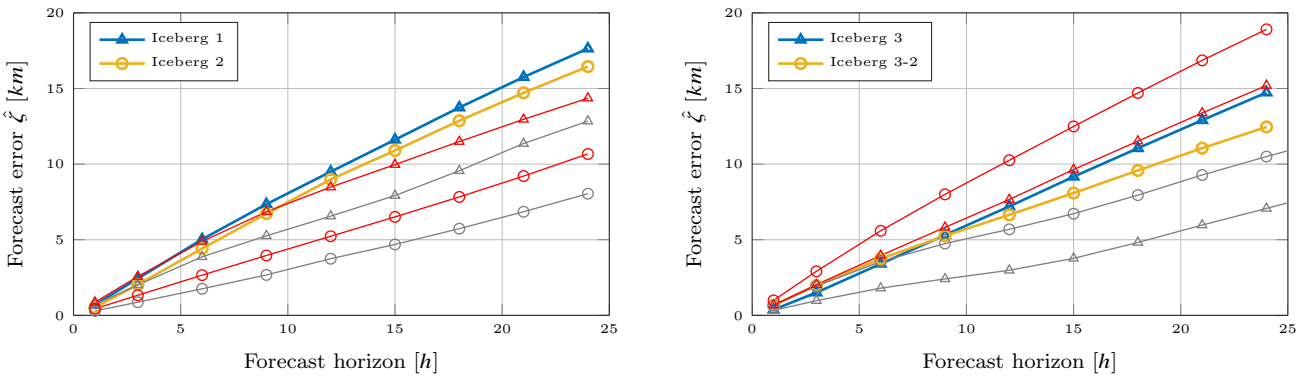

(a) Iceberg 1 and Iceberg 2 (b) Iceberg 3 and Iceberg 3-2

Figure 14: Forecast error $\hat{\zeta}$ for different forecast horizons for the dynamical (blue and yellow), stationary (red) and VAR model (gray).

For Iceberg 1, the elliptic iceberg keel shape works best. Overall, the performance is similar using the layered mean plus tidal current or the surface current. Only the error for Iceberg 3-2 reduced considerably using the surface current, which indicates the iceberg is most likely small and mainly driven by surface currents.

The best mean error $\hat{\zeta}$ for the entire iceberg trajectories available for different forecast horizons of each iceberg is shown in Figure 14. The stationary model assumes that the iceberg does not move. The error growth Γ of the dynamic, VAR and stationary models are shown in Table 2.

For Iceberg 1 and Iceberg 2 (Fig. 14a) the dynamic iceberg model produces worse results than assuming the icebergs are stationary. For Iceberg 1 this important performance boundary is reached for longer forecast horizons than 15 h. Iceberg 1 is the only iceberg where the boundary is reached within the 24 h forecast horizon. For Iceberg 3 (Fig. 14b), the dynamic iceberg model has a similar error change Γ as the stationary model (Table 2). In fact, both icebergs are close to shore so it is expected that the ocean current model may perform poorly and causes large forecast errors using the dynamic iceberg model.

For the short-term drift forecasts, the VAR model produces on average better forecast results than the dynamic

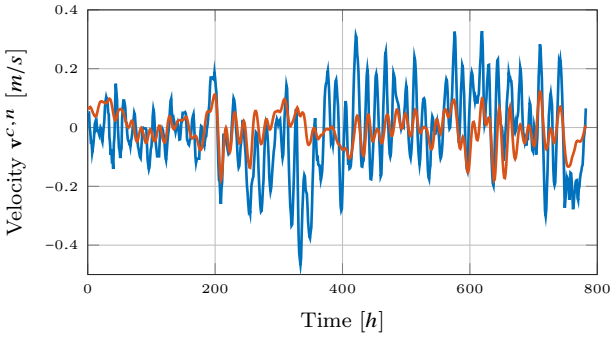

(a) North-south direction.

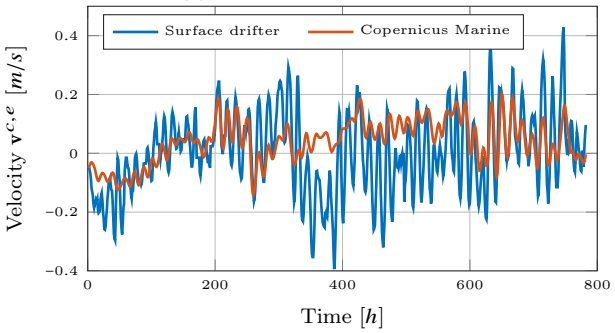

(b) East-west direction.

Figure 12: Example of the ocean current velocity calculated from the movements of one surface drifter and the ocean surface velocity from the Copernicus Marine webpage.

model. However, the tendency of the error change Γ for longer forecast horizons decreases for the dynamic iceberg model while increases for the VAR model indicating that there may be a crossing point in time after which the dynamic iceberg model performs better.

If the corrected current (Eq. 15) is used, then the forecast of Iceberg 2 and Iceberg 3 improves, worsens for Iceberg 3-2, and remains the same for Iceberg 1. The overall forecast performance improves slightly, but the VAR model forecast remains superior.

Even though the VAR model is on average superior for short-term forecasts, only the dynamic model can forecast rapid and sudden direction changes. This can be seen in Figure 15a where the iceberg makes a sudden "unexpected" (by the VAR model) change of direction. The VAR model was well-adjusted before the change, but was not able to predict the change. Even though the forecast is not very good, the dynamic iceberg model predicts a direction change. After the change of direction, the VAR model adjusts itself again, and its forecast improves.

On the other hand, it can happen that with the dynamic drift model, a direction change is predicted but not observed in the actual iceberg trajectory (Fig. 15b). In this example, the dynamic model forecast direction error is up to 180°.

The VAR forecast model can approximate curves and sometimes direction changes (Fig. 15c) and loops (Fig. 15d) if the observed dataset indicates these changes. For this, the cross-correlation term should be included in the model. The parts of the drift trajectories in Fig. 15 were chosen to support the discussion but we like to emphasise that they only show small parts of the total trajectories.

7.6. Relative performance index

The relative performance index κ provides a better index to compare different icebergs than an absolute performance index, such as the mean end position error $\hat{\zeta}$.

Using the VAR model Iceberg 3 shows the best relative performance κ (Fig. 16c). This correlates with the mean end position error $\hat{\zeta}$. However, the VAR model has a similar relative performance κ for Iceberg 2 (Fig. 16b) and Iceberg 3-2 (Fig. 16d), which is not obvious considering the mean end position error $\hat{\zeta}$ (e.g., 12 h forecast: Iceberg 2: $\hat{\zeta}$ = 9 km, Iceberg 3-2: $\hat{\zeta}$ = 6.6 km).

Overall, the change between forecast performance categories (excellent, good, acceptable, bad) over a changing forecast horizon is relatively small. This may be a useful property, which may help to categorise the performance of the forecast of an iceberg trajectory after a few hours. It is likely that this categorization is a good approximation also for longer forecast horizons.

8. Conclusion and Future Work

This article proposes a statistical approach to short-term iceberg forecasting. The basic premise is that the ocean current velocity can be estimated with help of a simple kinematic relationship between iceberg, wind and current velocities. Thereafter, the ocean current can be forecasted. The advantage of this transformation is that sufficient ocean current velocity data (modelled or measured) are available to identify a statistical ocean current model. Two interesting effects arise from this transformation: First, it is possible to identify a VAR ocean model for each grid cell allowing to include local specifics into the statistical iceberg forecast. Second, during the identification of the ocean current model, an error term is identified which may help to compute confidence regions of the iceberg drift forecast. However, this was not done in this article and it is recommended to use measured ocean current data that have high frequency components to approximate these confidence regions.

After the identification of a VAR current model, its applicability to iceberg forecasting was analysed and tested on four real iceberg drift tracks. It was shown that a VAR model order of $p = 3$ (see Eq. 3) is sufficient to forecast the iceberg drift. Since the VAR model is identified with modelled current data, and the iceberg forecast uses measured iceberg position data, a filter is necessary. If the cross-correlation between orthogonal current velocities was included in the model, then a shorter filter horizon of about 7 h to 10 h sufficed. If the cross-correlation was excluded, then a filter horizon of about 13 h to 15 h was necessary. The statistical approach can be used for a forecast up to at

least 12 h where a minimum error change Γ was observed. Longer forecast horizons t_h are possible, but usually larger error growth than before were observed. In comparison with the dynamic iceberg model, this statistical approach had superior performance for all tested iceberg drift tracks up to a forecast horizon of 24 h. Longer forecast horizons were not compared.

Even though the forecast approach performed well on the iceberg dataset we like to point out that a critical assumption in this work is to trust the wind forecast completely and to neglect the vertical variations in the current over the iceberg keel. The former will introduce an error if the wind is forecasted faulty. The latter may degrade the performance of the approach for large icebergs in areas subjected to strong current variations over the iceberg keel. On the other hand, even in these cases the approach is able to approximate the ocean current forcing and perform most likely a reasonable forecast. Clearly the approach has to be tested on differently sized iceberg in different areas in order to evaluate further how well the forecast approach works.

In addition, in the future the forecast approach should be tested using measured ocean current data to identify a statistical ocean current model. This will give a better knowledge how important it is to include fast dynamics into the model or if these dynamics have to be filtered. Furthermore, a distributed statistical ocean current and also other model identification methods may be tested. The approach even has the potential to be used with machine learning techniques. A comparison of drift forecast models identified by machine learning techniques and traditional statistical identification methods will be very interesting.

It may be also investigated if a similar performance as in this article can be achieved by directly identifying a statistical iceberg drift model. The training set for the model identification may be generated by running many different simulations with the dynamic iceberg model driven by a suitable ocean current and wind model.

References

Allison, K., Crocker, G., Tran, H., Carrieres, T., 2014. An ensemble forecast model of iceberg drift. Cold Regions Science and Technology 108, 1 – 9.

Andersson, L. E., Scibilia, F., Copland, L., Imsland, L., 2018. Comparison of statistical iceberg forecast models. Cold Regions Science and Technology 155.

Andersson, L. E., Scibilia, F., Imsland, L., 2016. An estimation-forecast set-up for iceberg drift prediction. Cold Regions Science and Technology 131, 88–107.

Andersson, L. E., Scibilia, F., Imsland, L., 2017. A study on an iceberg drift trajectory. In: ASME 2017 36th International Conference on Ocean, Offshore and Arctic Engineering. Vol. 8. American Society of Mechanical Engineers, pp. V008T07A029–V008T07A029.

ArcticNet, 2004-2018. [Online]. Available: www.arcticnet.ulaval.ca.

Barnett, L., Seth, A. K., 2014. The MVGC multivariate Granger causality toolbox: A new approach to Granger-causal inference. Journal of Neuroscience Methods 223, 50 – 68.

Bigg, G. R., Wadley, M. R., Stevens, D. P., Johnson, J. A., 1996. Prediction of iceberg trajectories for the North Atlantic and Arctic oceans. Geophysical Research Letters 23 (24), 3587–3590.

Bigg, G. R., Wadley, M. R., Stevens, D. P., Johnson, J. A., 1997. Modelling the dynamics and thermodynamics of icebergs. Cold Regions Science and Technology 26 (2), 113–135.

Broström, G., Melsom, A., Sayed, M., Kubat, I., Dec. 2009. Iceberg modeling at met.no: Validation of iceberg model. Tech. Rep. 17, Norwegian Meteorological Institute.

C-CORE, 2007. Ice management for structures in sea ice with ridges and icebergs. Volume 1 - state of the art in iceberg management. C-CORE Report R-07-037-544.

Egbert, G. D., Erofeeva, S. Y., 2002. Efficient inverse modeling of barotropic ocean tides. Journal of Atmospheric and Oceanic Technology 19 (2), 183–204.

EI-Tahan, M., EI-Tahan, H., Venkatesh, S., et al., 1983. Forecast of iceberg ensemble drift. In: Offshore Technology Conference.

Eik, K., 2009. Iceberg drift modelling and validation of applied metocean hindcast data. Cold Regions Science and Technology 57, 67–90.

Garrett, C., 1985. Statistical prediction of iceberg trajectories. Cold Regions Science and Technology 11 (3), 255 – 266.

Garrett, C., Middleton, J., Hazen, M., Majaess, F., 1985. Tidal currents and eddy statistics from iceberg trajectories off Labrador. Science 227 (4692), 1333–1335.

Granger, C. W., 1969. Investigating causal relations by econometric models and cross-spectral methods. Econometrica: Journal of the Econometric Society, 424–438.

Kubat, I., Sayed, M., Savage, S., Carrieres, T., Crocker, G., 2007. An operational iceberg deterioration model. In: Proceedings of the Sixteenth (2007) International Offshore and Polar Engineering Conference. pp. 652–657.

Kubat, I., Sayed, M., Savage, S. B., Carrieres, T., 2005. An operational model of iceberg drift. International Journal of Offshore and Polar Engineering 15 (2), 125–131.

Kulakov, M. Y., Demchev, D. M., 2015. Simulation of iceberg drift as a component of ice monitoring in the West Arctic. Russian Meteorology and Hydrology 40 (12), 807–813.

Marko, J., Fissel, D., Miller, J., 1988. Iceberg movement prediction off the Canadian east coast. In: El-Sabh, M., Murty, T. (Eds.), Natural and Man-Made Hazards. Springer Netherlands, pp. 435–462.

Moore, M., 1987. Exponential smoothing to predict iceberg trajectories. Cold Regions Science and Technology 14 (3), 263 – 272.

Mountain, D., 1980. On predicting iceberg drift. Cold Regions Science and Technology 1 (3-4), 273 – 282.

Smith, S. D., 1993. Hindcasting iceberg drift using current profiles and winds. Cold Regions Science and Technology 22 (1), 33–45.

Smith, S. D., Donaldson, N. R., 1987. Dynamic modelling of iceberg drift using current profiles. Fisheries and Oceans, Canada.

Sodhi, D., El-Tahan, M., 1980. Prediction of an iceberg drift trajectory during a storm. Ann. Glaciol 1, 77–82.

Turnbull, I. D., Fournier, N., Stolwijk, M., Fosnaes, T., McGonigal, D., 2015. Operational iceberg drift forecasting in northwest Greenland. Cold Regions Science and Technology 110, 1 – 18.

Ur Rehman, N., Mandic, D. P., 2010. Multivariate empirical mode decomposition. In: Proceedings of The Royal Society of London A: Mathematical, Physical and Engineering Sciences. Vol. 466. The Royal Society, pp. 1291–1302.

Wagner, T. J., Dell, R. W., Eisenman, I., 2017. An analytical model of iceberg drift. Journal of Physical Oceanography 47 (7).

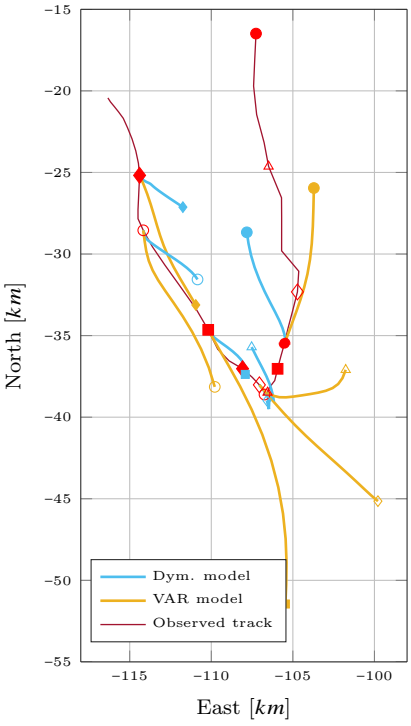

(a) Example 1

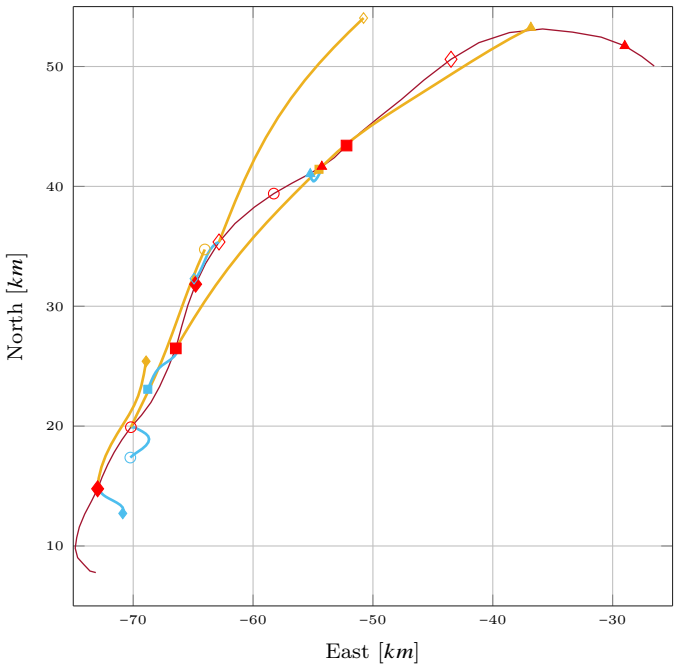

(b) Example 2

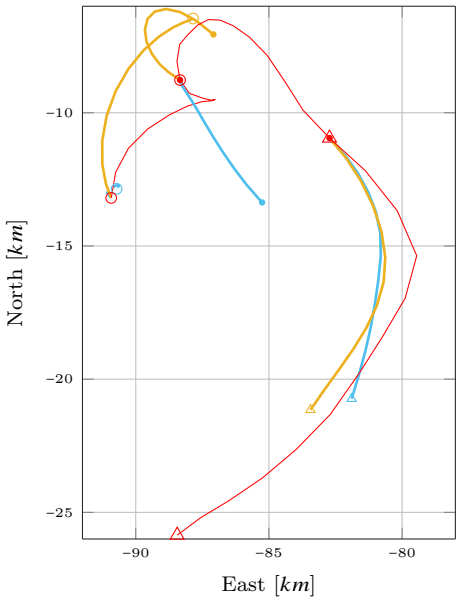

(c) Example 3

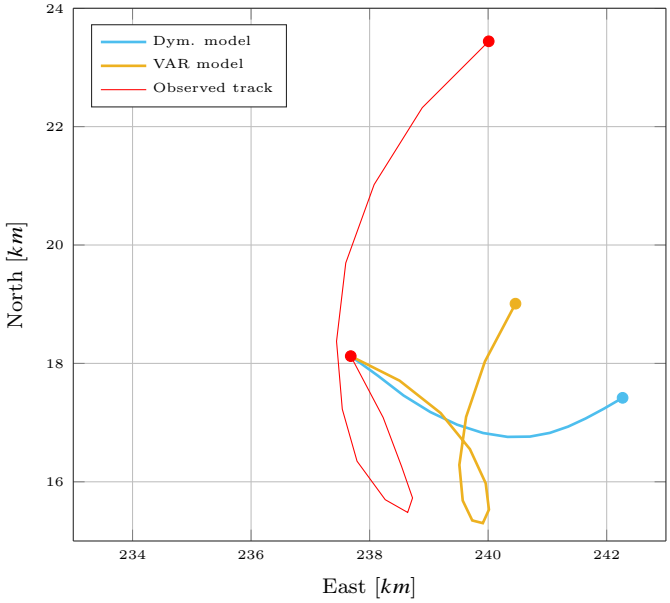

(d) Example 4

Figure 15: Several forecast examples for the VAR and dynamical iceberg model to support the discussion. The red line shows the observed iceberg trajectory. The initial and end point of each 12 h forecast are marked with the same markers on the observed and forecasted iceberg trajectory.

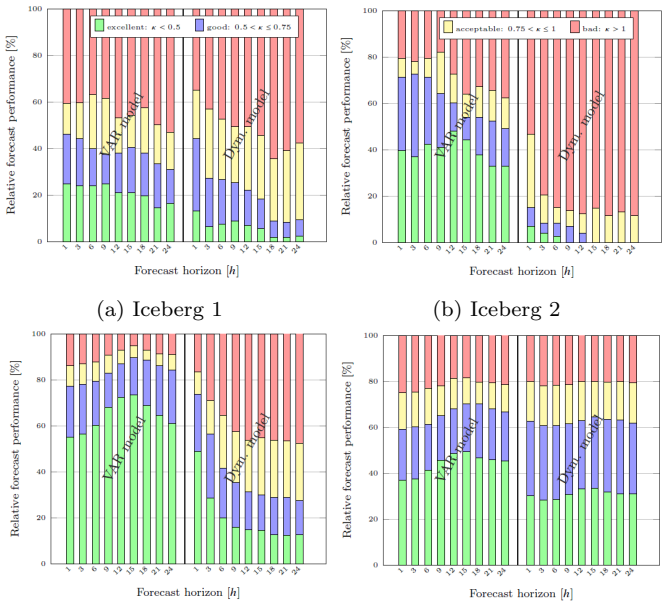

(a) Iceberg 1 (b) Iceberg 2

(c) Iceberg 3 (d) Iceberg 3-2

Figure 16: Relative forecast performance of the entire trajectory of Iceberg 1, 2, 3, and 3-2. The relative forecast performance is grouped in four categories (Sec. 4): bad (red), acceptable (yellow), good (blue), excellent (green). Each iceberg forecast performed is grouped in one of the categories. Each vertical bar shows the percentage of each category for a certain method and forecast horizon. The performance of the VAR model is on the left-hand side and the right-hand side of a dynamic model.